

AD-A154 041

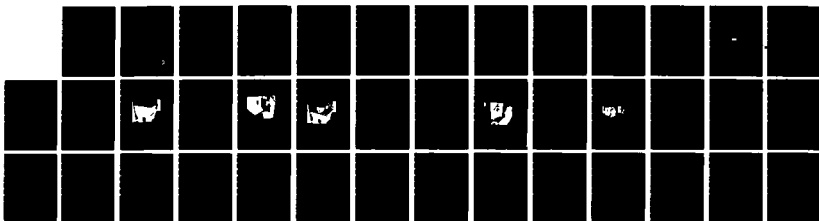
COMPOSITE MATCHED FILTERS(U) AERODYNE RESEARCH INC
BILLERICA MA JUL 82 ARI-RR-310 DAAH01-82-C-A173

1/1

UNCLASSIFIED

F/G 20/6

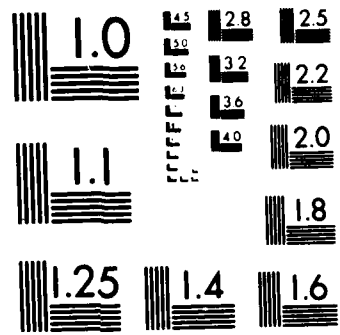
NL



END

FILMED

DTIC



MICROCOPY RESOLUTION TEST CHART
NATIONAL BUREAU OF STANDARDS 1963 A

①

AD-A154 041

COMPOSITE MATCHED FILTERS

Prepared by:

Aerodyne Research, Inc.
45 Manning Road
Billerica, MA 01821

Prepared for:

Commander, U.S. Army Missile Command
G&C Directorate, Building 5400
Attn: DRSMI-RR0/Duthie
Redstone Arsenal, AL 35898

Final Technical Report

Prepared under Contract No. DAAH01-82-C-A173

July 1982

DTIC
ELECTE
MAY 21 1985
S D

B

DISTRIBUTION STATEMENT A
Approved for public release
Distribution Unlimited

DTIC FILE COPY

TABLE OF CONTENTS

<u>Section</u>		<u>Page</u>
	EXECUTIVE SUMMARY	
1	INTRODUCTION	1-1
2	EQUIPMENT AND EXPERIMENTAL DESIGN	2-1
	2.1 Introduction	2-1
	2.2 Recording Media	2-1
	2.3 Hardware Considerations	2-3
	2.4 Readout Considerations	2-14
3	THEORETICAL ANALYSIS	3-1
4	EXPERIMENTAL RESULTS	4-1
	4.1 K-Ratio and Dynamic Range	4-1
	4.2 Repeatability	4-1
	4.3 Additivity	4-2
	4.4 Subtraction	4-2
5	CONCLUSIONS	5-1
6	REFERENCES	6-1

APPENDIX
COMPONENTS LIST

Accession For	
NTIS	<input checked="" type="checkbox"/>
DTIC	<input type="checkbox"/>
Unannounced	<input type="checkbox"/>
PER LETTER	
Availability Codes	
Special	
A-1	

LIST OF ILLUSTRATIONS

<u>Figure</u>		<u>Page</u>
1.1	Program Outline	1-2
1.2	Recording Geometry	1-4
1.3	Tank Image	1-7
2.1	H-D Curves of High Resolution Plates	2-2
2.2	Table Cover Built to Minimize Air Currents	2-4
2.3	Beamsplitter (Right), Liquid Gate (Left)	2-6
2.4	Assembly Plate Used to Avoid Mechanical Motions	2-7
2.5	Shutter	2-9
2.6	Plate Holder (Mid Center) with Retaining Cap (Lower Center)	2-10
2.7	Plate Used for Precise Longitudinal Multipositioning of the Input Image	2-12
4.1	Typical Additivity Result	4-3
4.2	Typical Subtraction Result	4-4

EXECUTIVE SUMMARY

In a paper and in the proposal we showed that the power of computer optimization could be combined with the good features of optical matched filters by constructing composite matched filters of the form:

$$\text{CMF}(u,v) = c_1 \text{MF}_1(u,v) + c_2 \text{MF}_2(u,v) + c_N \text{MF}_N(u,v),$$

where c_1, c_2, \dots, c_N are real computer-optimized weights and $\text{MF}_1, \text{MF}_2, \dots, \text{MF}_N$ are a basis set of matched filters. This report covers our attempt to synthesize those filters optically.

The basic strategy is simple.

1. Make the basis set $\text{MF}_1, \text{MF}_2, \dots, \text{MF}_N$ optically,
2. Characterize the basis set of filters using various input patterns,
3. Using the resulting data, computer optimize c_1, c_2, \dots, c_N ,
4. Record CMF using exposure times proportional to $|c_1|, |c_2|, \dots, |c_N|$ for the various MF's and using a half wave plate to vary the sign of the c's.

Test the resulting CMF what we found experimentally is that actually accomplishing this task is beyond the state-of-the-art. The reasons, in retrospect, are perfectly clear. The program outlined in ~~steps 1-4~~ places much more severe strains on the equipment and materials than has ever been placed by ordinary holography. Barely-acceptable repeatability of MF's was achieved with great effort, but additivity of MF's failed completely. That is, the nonlinearities of holography came to dominate CMF synthesis. In this report we trace the problems encountered, show why no directly-useful holograms can be obtained with state-of-the-art equipment, and indicate the equipment requirements for the eventual successful application of the CMF concept.

1. INTRODUCTION

It has been known for many years¹ that optical pattern recognition filters superior to matched filters could be computed. A great deal of recent activity has been devoted to devising methods of using the power of the digital computer to derive masks which could only be written by computer.²⁻¹¹ Such holograms, however, have several characteristic drawbacks. First, hologram writers capable of recording these filters to sufficient accuracy have only recently become available. Second, such holograms usually have a very limited information content. It is typical that such a hologram might operate on a 512 x 512 array sample of the Fourier transform of the input object. This contrasts with an optical hologram which might have effectively 10,000 x 10,000 Fourier transform samples. Third, the diffraction efficiency of a computer generated hologram is generally very poor. Fourth, real optical systems seldom produce an exact Fourier transform. Accordingly, filters generated on the assumption of Fourier transformation may not work as well in the real optical system as they do in the computer analysis. For all of these reasons, we have suggested in a previous paper¹² that a multiple exposure matched filter or "Composite Matched Filter" be considered. The composite matched filter (CMF) would be a linear sum of optically exposed matched filters. The weights in the linear combination would be computer optimized on the basis of experiments done with single exposure matched filters. This contract was intended to explore the experimental feasibility of this technique for combining the power of the computer with the good features inherent in an optical matched filter.

Accordingly, Aerodyne Research, Inc. (ARI) outlined a systematic experimental program as outlined in Figure 1.1. Here we review those steps one by one.

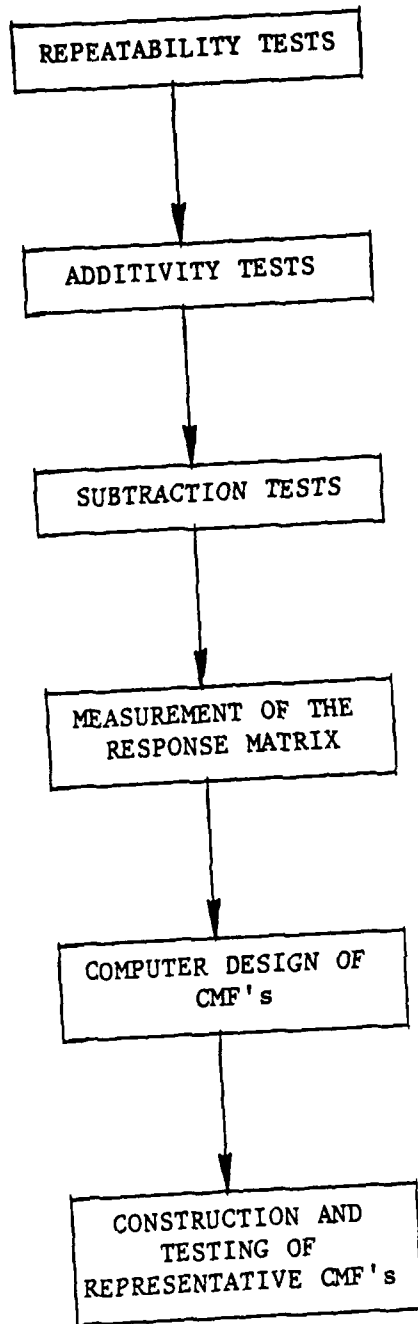


Figure 1.1 Program Outline

• Repeatability tests are clearly the key step. In its simplest form, the question is: "Can we make two identical optical holographic matched filters?" Here are the primary reasons this question is so important.

1. Any militarily-useful system must be repeatable.
2. The CMF production strategy calls for making MF's, measuring their behavior, choosing weights which give a desirable composite behavior, and synthesizing the resulting filter by multiple exposure holography. Each of the multiple exposures must lead to a highly predictable result for this strategy to be realized.

It is by no means a "given" that repeatability is achievable.

EE

In order to test stability, we required a definition of the quantity under test. We used as a measure of the pattern recognition effectiveness of the hologram the fraction of the incident power in the object beam which is diffracted onto the correlation spot. Figure 1.2 shows the recording geometry schematically. Reinserting the recorded hologram in place and striking it with the object beam alone produces a reconstructed version of the reference beam. Focusing the reconstructed beam down to a point produces a correlation spot. We then insert a small detector in the correlation spot to measure the "autocorrelation signal". The question we addressed was whether the autocorrelation signal could be repeated from one hologram to the next. Therefore, what we did was detect the light intensity coming into the object transparency as well as the signal falling in the detector region and directly, electronically, ratio the readings to obtain the reading $S_{i,j}$. By $S_{i,j}$ we mean the reading obtained with the i^{th} input image when the j^{th} hologram is present. The important question that we have to ask is "How repeatable is $S_{i,j}$?" For initial tests, it was sufficient to pick a single $S_{i,i}$ and ask what repeatabilities were obtained. We then went on to test the stability of $S_{i,j}$ readings. Repeatability and stability are words that both imply constancy while some other factors are varying. We now list the variables that might lead to differing values of tests of $S_{i,j}$.

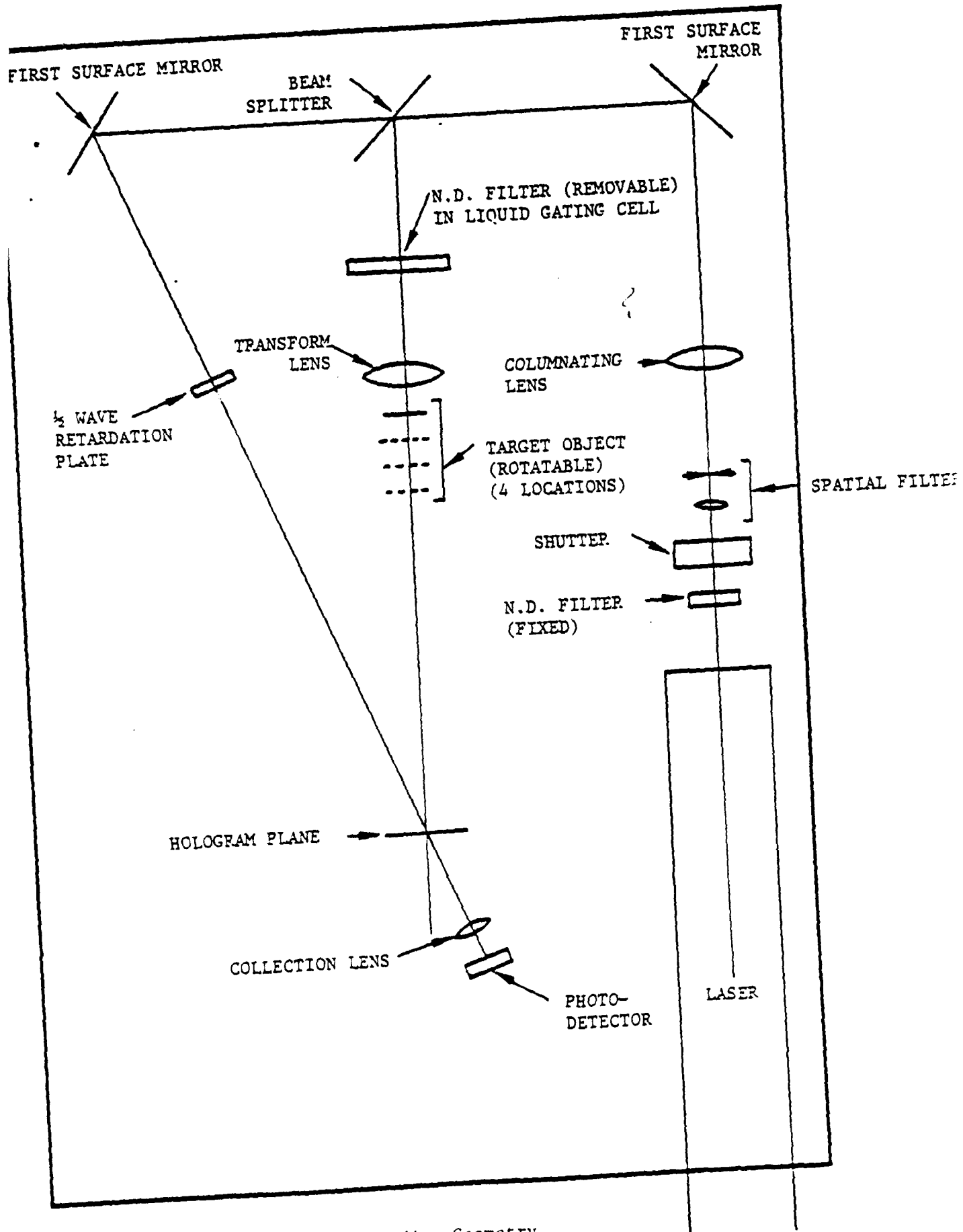


Figure 1.2. Recording Geometry

(1) Photographic Variations

Photographic variations can occur either because successive photographic plates are not identical or because the processing is not identical on successive plates.

(2) Geometric Variations

It is perfectly reasonable to believe that simply picking up the hologram and replacing it in its holder may align it differently. This will lead to a different value of $S_{i,j}$. Likewise, removing the input transparency and replacing it could also lead to such a variation. Finally, the combination of reinsertion of the input transparency plus rotation of that transparency may lead to a characteristic amount of misalignment and hence variability in $S_{i,j}$.

(3) Exposure Variations

It is perfectly possible that successive exposures may be different in either total exposure or in the spatial distribution of the exposing radiation. This too can lead to variability in $S_{i,j}$.

(4) Ageing

Strickly speaking, ageing is not a possible cause for variation in $S_{i,j}$. Rather, ageing is simply a process or a recipe whereby variations of many kinds can be allowed to occur. As the hologram sits on the shelf it may undergo slow photochemical reactions. It may undergo physical changes as the emulsion swells and retracts in response to temperature and humidity changes.

(5) Use Environment

It may be that such factors as the temperature and humidity of the room during the use effect $S_{i,j}$.

Additivity Tests are designed to test experimentally the possibility that if we can make two matched filters MF_1 and MF_2 , we can make a composite matched filter

$$CMF = c_1 MF_1 + c_2 MF_2$$

(where c_1 and c_2 are positive) which has the behavior expected from our knowledge of MF_1 and MF_2 .

Measurement of the Response Matrix calls for determining a complete set of $S_{i,j}$'s for the range of images of interest. The images were all rotated and magnified versions of the tank image shown in Figure 1.3.

Computer Design of CMF's is a simple operation given the $S_{i,j}$'s, because the hard work has been done before.¹²

Construction and Testing of Representative CMF's would complete a laboratory demonstration of CMF feasibility.

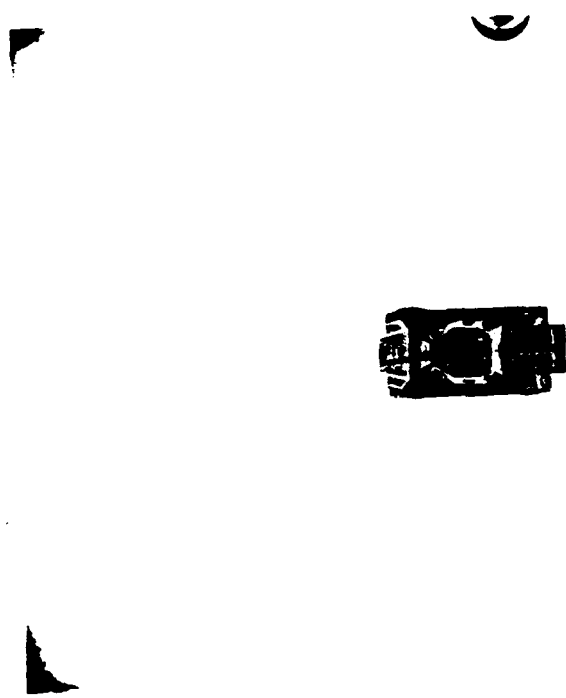


Figure 1.3 Tank Image

2. EQUIPMENT AND EXPERIMENTAL DESIGN

1 Introduction

Regarding repeatability as the primary possible problem, we went to great lengths to eliminate ahead of time many sources of nonrepeatability. The basic system followed the design of Figure 1.2. We turn now to actual design choices. A component list is given in the Appendix.

2 Recording Media

In our experiments we restricted ourselves to the most readily available coding media - photographic plates. Eastman Kodak High Resolution Plates were chosen because they had sufficient resolution to record good holograms, they were readily repeatable with regard to the exposure versus density curve. Like most holographic plates, these have a high degree of linearity. Figure 2.1 shows a typical density versus log E curve or H-D curve. Over a suitable range of exposures the density is proportional to the logarithm of the exposure. The slope of that curve is called γ . Thus in that region we can write

$$D = D_0 + \gamma \log E \quad . \quad (2-1)$$

Using the error in exposure δE and the error in density δD , we have $\delta D = \gamma \delta E / E$.

$$\delta D = \gamma \delta E / E \quad . \quad (2-2)$$

For low D_0 , we have

$$\frac{\delta D}{D} \approx \frac{\gamma \delta E}{E^{\gamma+1}} = \left(\frac{\delta}{E} \right) \frac{\delta E}{E} \quad . \quad (2-3)$$

The intensity of the reference and object beams individually are $|R|^2$ and $|O|^2$. In holography one speaks of the K ratio

$$K = \frac{|R|^2}{|O|^2} \quad (3-2)$$

Thus

$$\frac{I}{|O|^2} = K + 1 + 2\sqrt{K} \cos \phi \quad (3-3)$$

Using the accepted definition of the depth of modulation

$$DOM = \frac{I_{\max} - I_{\min}}{I_{\max} + I_{\min}} \quad (3-4)$$

we have

$$DOM = \frac{2\sqrt{K}}{K+1} \quad (3-5)$$

The exposure is

$$E = It \quad (3-6)$$

where t is the exposure time.

The amplitude transmission of the hologram at the point depends not only on I but also on the response characteristics of the recording medium. For exposures in the so called "linear" region of an ideal photographic medium, the amplitude transmission is

3. THEORETICAL ANALYSIS

The problem we address is whether, in principle, it is possible to form the composite matched filter as was suggested in both the paper and the proposal. We suppose that we have a hologram set up in which the object information can be changed while leaving the reference information identical. Suppose we have objects $O_1(x,y)$ and $O_2(x,y)$. We insert them successively in the object beam to form matched filters $MF_1(u,v)$ and $MF_2(u,v)$. Both holograms are supposed to have resulted from exposures for a duration t_0 . The hypothesis is that by exposing for time one half t_0 to object O_1 and time one half t_0 to object O_2 , we arrive at a composite matched filter

$$CMF = (1/2) MF_1 + (1/2) MF_2 .$$

There are, in fact, many hidden assumptions in this hypothesis. For our purposes, we will content ourselves with a thin hologram analysis. Thick holograms offer more complication of analysis and even less opportunity for the desired linearity.

In discussing the diffraction efficiency of thin holograms, we must first calculate the optical interference pattern available for recording and then calculate the effect of the recording material. At each point in the hologram plane there is a reference beam and an object beam. Let us confine ourselves to each such point and call the scalar amplitudes of the two beams R and O . Assuming perfect coherence, the optical intensity pattern is proportional to:

$$\begin{aligned} I &= |R + O|^2 \\ &= |R|^2 + |O|^2 + 2 |R| |O| \cos \phi \end{aligned} \quad (3-1)$$

where ϕ is the phase angle between the two beams.

2.4 Readout Considerations

In readout we:

- o Reinsert the hologram accurately in its taking position,
- o Place a lens in the reference beam,
- o Place a pinhole at the focus of the reference beam,
- o Block the reference beam,
- o Remove all neutral density filters from the object beam, and
- o Measure the power of the light diffraction from the object beam through the pinhole as the object transparency is translated and rotated.

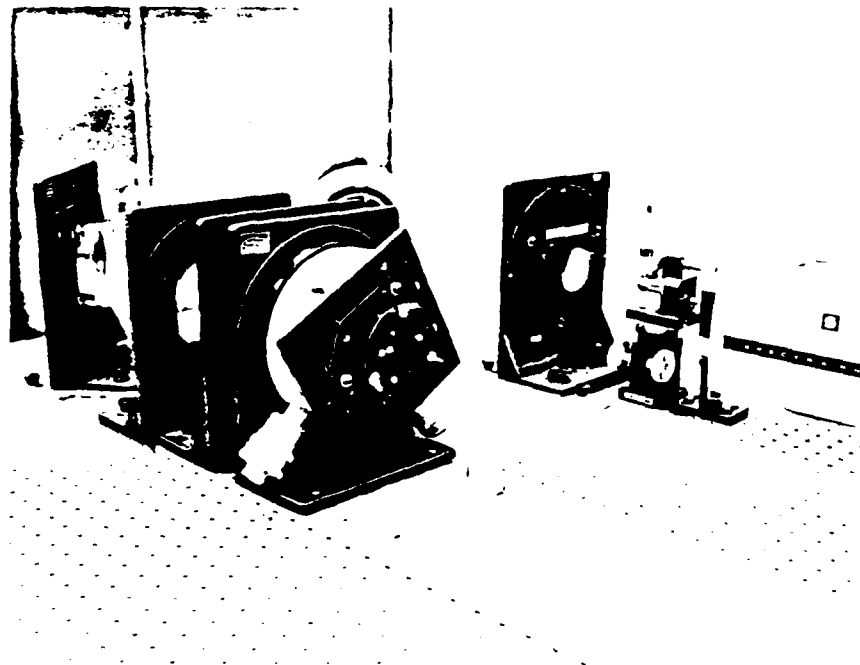


Figure 2.7 Plate Used for Precise Longitudinal Multipositioning of the Input Image

the size of the smallest fringe. That fringe will be diffraction limited. For the systems we are using, the smallest fringe should be no smaller than 4 to 5 microns. Accordingly, this relocation accuracy is not a major concern.

(h) Halfwave Plate

It was our intent to accomplish subtraction by use of a halfwave plate. By aligning the polarization of the laser beam along one axis we do not affect the polarization of the light. By rotating the halfwave plate 90°, we align the polarization with the other axis of the halfwave plate. The optical path differences between those two axes are designed to be exactly half a wave at 0.5145 μm. We were able to verify that rotating the halfwave plate did not shift the object beam. However, it did produce a totally unexpected and unacceptable side effect. The power transmission of the halfwave plate varied with orientation. This is a fairly subtle effect (< 5%). Nevertheless, it means that we cannot accurately subtract one hologram from the other to that accuracy. By adjusting the exposure levels properly, we could achieve 2% or better subtraction accuracy as measured from CMF's of the form:

$$CMF = 0.5 MF_1 - 0.5 MF_2$$

(i) Image Scale and Angle Control

We placed the transparency of the tank (roughly 0.5 cm) in a converging beam. By varying the distance between the transparency and the focal point, we varied the scale of the Fourier transform and therefore the effective image size. Repeatable positioning was achieved by relocation pins designed to exactly fit holes in the carrier plate (Figure 2.7). Care was taken to assure that the centroid of the tank stayed on axis.

Rotation was achieved by a micrometer adjustable stage capable of ±5 minute resetting which was afixed to the carrier plate. The tank centroid (judged not measured) was centered on the axis of the converging beam.

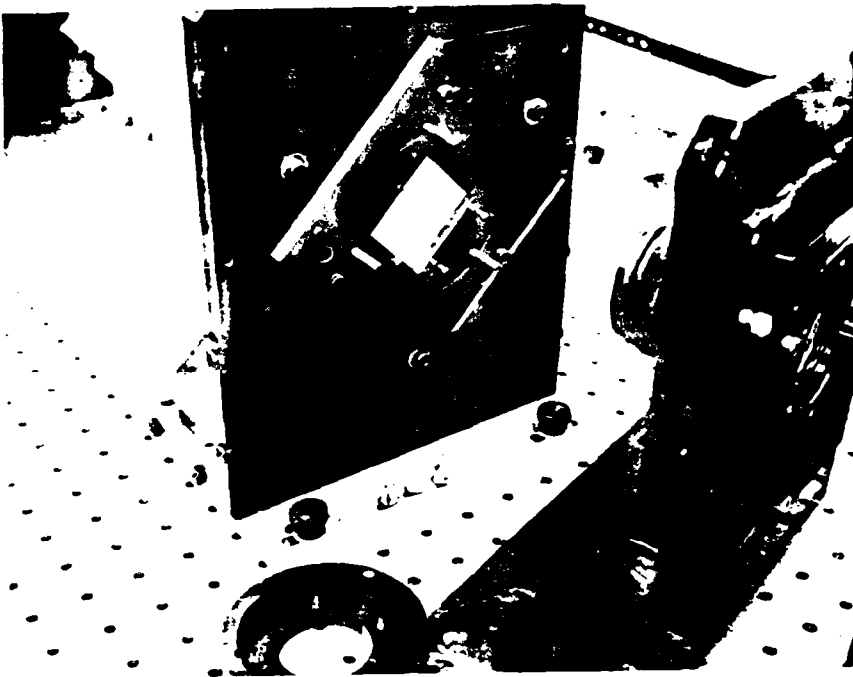


Figure 2.6 Plate Holder (Mid-Center) with Retaining Cap (Lower Center)

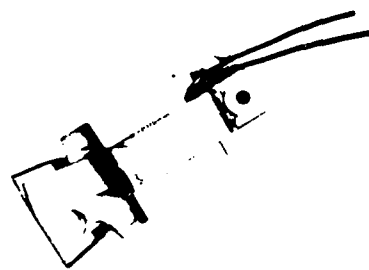


Figure 2.5 Shutter

(e) Shutter

We used a commercial electronic shutter manufactured by Newport Research Corporation. This shutter is simply a solenoid activated blade as pictured in Figure 2.5. The electronic controls provided allowed the exposure time to vary from 10 milliseconds to 99 seconds in steps as small as 7 milliseconds. By observing the detected beam on an oscilloscope, we were able to show that the shutter functioned reliably to 1% or better accuracy in all cases except for a rapid succession of exposures. With at least a half second wait between exposures, essentially perfect functioning was obtained at all times.

(f) Neutral Density Filters

In adjusting the beam ratio, it was necessary to introduce neutral density filters into the beam. Again this offered no problem whatever in recording single holograms on single days. On the other hand, however, it offered a major problem in situations in which the neutral density filter must be removed and subsequently replaced. It turns out that commercial neutral density filters are not optically flat. This means that unless they are replaced in precisely the same position, their wedge and curvature will distort the beam in a different way each time. The final approach adopted was to use gelatin neutral density filters in a liquid gate to obtain repeatability. Figure 2.3 shows the gate we built for this purpose.

(g) Plate Holder

In order to guarantee replacement of the plates in precisely the same position for readout as was used in taking, we needed a high accuracy plate holder. We used a kinematic edge mount with three pins and gravity loading for lateral positioning and three balls with pressure loading for longitudinal positioning. Figure 2.6 shows the plate holder. This was shown to be accurate enough to allow real time zero fringe conditions for live fringe holography. Accordingly it was deemed accurate enough for relocation of the spatial filters. Actually, the relocation accuracy ought to be governed by

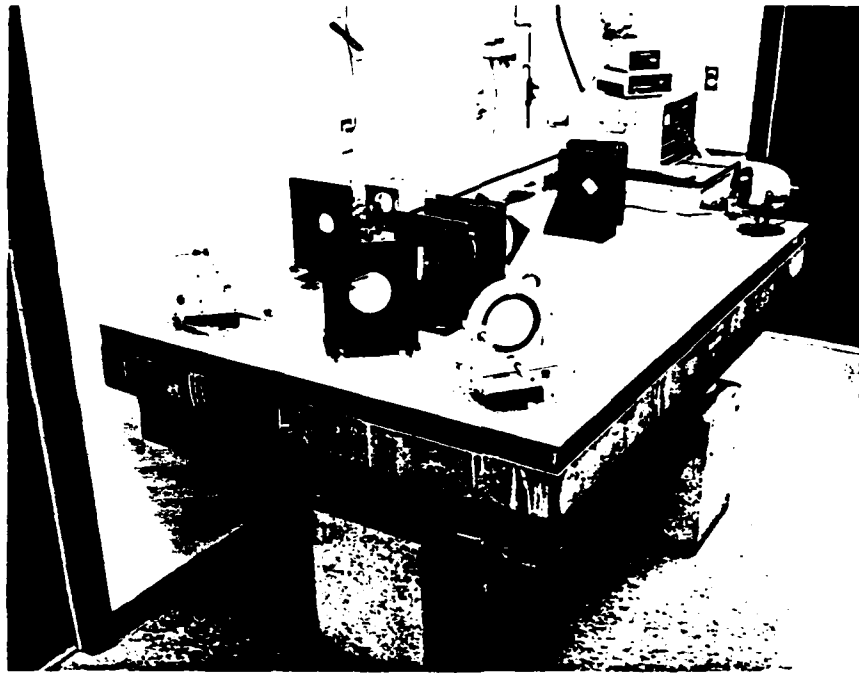


Figure 2.4 Assembly Plate Used to Avoid Mechanical Motions

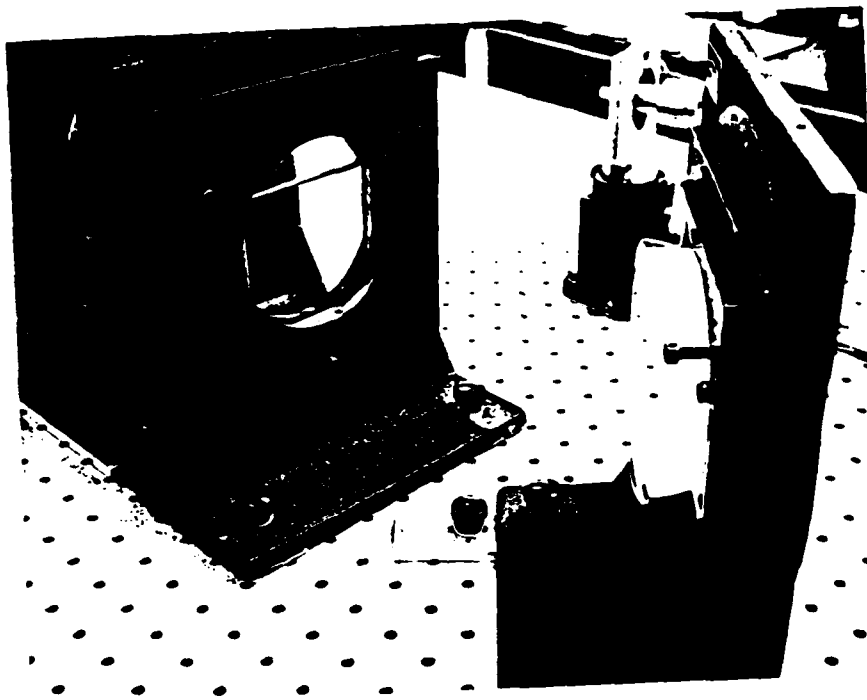


Figure 2.3 Beamsplitter (Right), Liquid Gate (Left)

the outside air temperature, and whether any openings were left in the cover. Of course, openings which tended to equilibrate inside and outside air temperatures also resulted in air flow which defeated the purpose of the cover. Our final conclusion is that we were better off with the cover on and closed than with any other condition.

(b) Spatial Filters

We employed spatial filters to clean up the laser beam. These had to be made of thin materials in order to function properly, but most thin materials simply melted in the focused laser beam. Our final approach was to go to a 25 μm tantalum pinhole.

(c) Beamsplitter

We found that the heat of the laser beam provided a slow and unpredictable physical change in the beamsplitter. This caused changes in the direction and curvature of the beam. While these changes were not detectable over a period of an hour, they were quite noticeable over a period of several hours or days. The best solution we were able to find was to place the beamsplitter in such a position that it encountered an expanded laser beam. While this did not altogether alleviate the problem, it brought that problem down to the scale of all other problems encountered during this task. Figure 2.3 shows the beamsplitter used and Figure 1.2 shows the overall system diagram and indicates where the beamsplitter is inserted.

(d) Physical Motion of the Components

In order to minimize physical motion of the various optical components we utilized a honeycombed assembly plate on top of the granite hologram plate. The assembly plate was provided with a regular array of tapped holes which we then utilized to clamp the components in place as indicated in Figure 2.4. So far as we could determine these components stayed in place during the entire three month experimental effort.

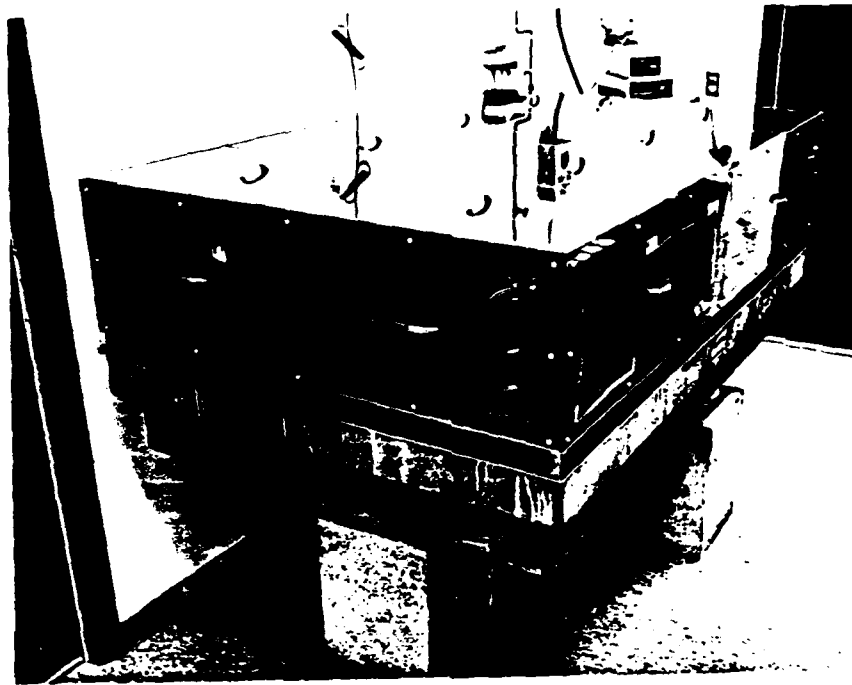


Figure 2.2 Table Cover Built to Minimize Air Currents

It is this variability in density that controls the hologram behavior. Because holographic recording media have high gamma, the effect of a small error in exposure is substantially magnified. That is, to achieve a 1% accuracy in the hologram, we must achieve substantially better than 1% accuracy in the exposure. Furthermore, bleaching the hologram has been observed in the course of these experiments to further increase the sensitivity of the diffraction efficiency to exposure. Thus two holograms which behaved in substantially identical manner before bleaching became quite different after bleaching. We concluded the only reasonable hope for achieving a high degree of repeatability is to use an unbleached holographic plate.

Of course all of this is predicated on keeping the development procedure as constant as possible. Accordingly, we took the following precautions:

- (1) Mix fresh developer every day,
- (2) Carry out all operations at a controlled temperature to within 1°C,
- (3) Time all development steps to control developing, and
- (4) Never reuse any photographic chemicals.

We experimented with a number of developers for repeatability and found that the best repeatability was obtained with Kodak D-76 (1-1) developing at 75°F for 7 minutes. Harsher developers like Kodak D-19 were tried but did not give as high a degree of repeatability.

2.3 Hardware Considerations

(a) Environment

We found that day to day repeatability was affected by air currents. To combat this we built a cover for the holographic table as shown in Figure 2.2. This, in turn, caused other problems. The air temperature inside became a function of the laser power, how long the laser had been on,

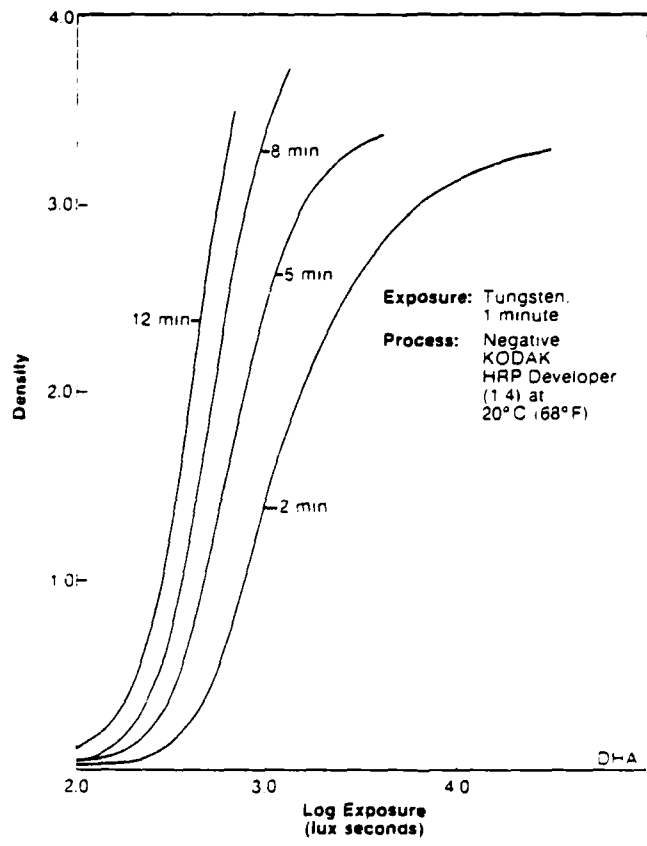


Figure 2.1 H-D Curves of High Resolution Plates

$$T = |E|^{-\gamma/2} \quad (3-7)$$

Here γ is the empirical slope of the density versus log E curve. This expression holds only over a particular range of exposures or densities. Outside of that range (either lower or higher exposures), the density varies little with exposure. Accordingly there is only a narrow operating range in photographic material and in that range the transmission versus exposure is closely approximated by the expression just given. For $\gamma = -2$, the depth of modulation of the hologram (in terms of the amplitude transmission) is equal to the depth of modulation of the recorded intensity pattern. For an inclined reference beam the phase of the reference beam varies linearly with position across the plate. This results, in general, in a net phase angle ϕ which varies as a function of position across the plate. For the particular case in which the object beam is also a plane wave, ϕ varies linearly across the plate. Thus for a $\gamma = -2$ hologram of two plane waves, we have a spatial cosine wave of amplitude proportional to $2\sqrt{K}$ plus a bias term of amplitude proportional to $K^2 + 1$. The cosine diffraction grating produces two orders (plus one and minus one) with amplitudes proportional to half the amplitude of the cosine term, or simply \sqrt{K} . The amplitude of the undiffracted light is proportional to $K + 1$. The detected intensity of either first order beam divided by the detected intensity of the zero order beam is called the diffraction efficiency, η . Thus,

$$\eta = \frac{K}{(K+1)^2} \quad (3-8)$$

Differentiating this expression and seeking its maximum, we find that the maximum value of the diffraction efficiency occurs for $K = 1$. The value of our expression for $K = 1$ is 0.25. For other reasons readily explained,*¹ the

*H.J. Caulfield and S. Liu, The Applications of Holography (Wiley Interscience, New York, 1968).

attainable diffraction efficiency is not 25% but 6.25%. Thus the exact expression for the diffraction efficiency is

$$\eta = \frac{K}{4(K+1)^2} \quad (3-9)$$

The other, and more common, special case is $\gamma = 2$ (a positive γ indicates the normal negative working recording). The direct argument from the equations as to why transmission proportional to E^{-1} behaves in a manner similar to a transmission proportional to E is quite complex. On the other hand, the physical argument is much easier to make. Physically, what we have is a hologram which is identical to $\gamma = -2$ hologram except that everywhere the prior hologram was dark this is transparent and conversely. This, then, is the hologram that we would have recorded with the identical set up but with a halfwave shift in one of the two beams. For $|\gamma|$ not equal to 2, the situation rapidly becomes more difficult to analyze.

With this small review of the recording terminology, we are in a position to assess some of the problems associated with composite matched filters. The first of those has to do with the diffraction efficiency. It is normally the case that optical matched filters are recorded with the K ratio at the center of the Fourier transform one or less. For the K ratio less than one, we emphasize that range of spatial frequencies which corresponds to $K = 1$. It is not at all uncommon that such a hologram have a diffraction efficiency of around 1%. If we seek to record a multiple exposure hologram in which the available dynamic range is shared equally among N independent holograms with non-overlapping images, the maximum diffraction efficiency of each is the maximum diffraction efficiency of a single hologram divided by N^2 .¹³ This factor of N^2 occurs for two reasons. First, the incident light must be shared equally among the N wavefronts accounting for a factor of $1/N$. That is, there can be no preference among the recorded wavefronts as to which gets the reconstructing energy. Second, the available dynamic range must be shared

among the N separate exposures resulting in another factor of 1/N loss. That is, a diffraction pattern for one of the N holograms can have a depth of modulation of at most 1/N. In our case, previous theory for non-overlapping images does not apply.

We now derive a more general case. Let MF_1 be formed by interfering beams R_i and O_i . By assumption R_i is a positive constant $R = |R|$. Let the exposure time be t_i . Then the exposure pattern is

$$E = \sum_i t_i |R + O_i|^2 = \sum_i t_i |R|^2 + \sum_i t_i |O_i|^2 + 2 \sum_i t_i R O_i^* \cos \phi_i. \quad (3-10)$$

For $\gamma = -2$ recording, the first order amplitude of the reconstructed wave is

$$O_1 = R \sum_i t_i O_i^* \quad (3-11)$$

That is, the t_i 's serve as the CMF weights. The diffraction efficiency of O_1 is

$$\eta_1 = \frac{R^2 \sum_i t_i^2 |O_i|^2}{\left[(\sum_k t_k R)^2 + \sum_k t_k |O_k|^2 \right]^2} \quad (3-12)$$

Writing

$$K_1 = R^2 / |O_1|^2 \quad (3-13)$$

K

we have

$$\eta_1 = \frac{t_1^2 K_1}{\left[k_1 \left(\sum_k t_k \right) + \sum_k t_k \left| O_k / O_1 \right|^2 \right]^2} \quad (3-14)$$

For $|O_k| = |O_1|$ independently of K,

$$\eta_1 = \frac{t_1^2}{\sum_k t_k} \frac{K_1}{(1+K_1)^2} = \left(\frac{t_1}{\sum_k t_k} \right)^2 \frac{K}{(1+K)^2} \quad (3-15)$$

Of course if $t_1 = t_2 = \dots = t_N = t_0/N$, then

$$\eta_1 = \frac{t_0^2/N^2}{t_0} \frac{K}{(1+K)^2} = \frac{K}{N^2 (1+K)^2} \quad (3-16)$$

as was proved many years ago.¹³

These individual diffraction efficiencies apply only when the individual images do not overlap. When they do overlap, we must calculate the diffraction efficiency η_1 of the whole composite wavefront O_1 . Thus

$$\eta_1 = \frac{R^2 \left| \sum_i t_i O_i \right|^2}{\left[\left(\sum_i t_i \right) R^2 + \sum_i t_i \left| O_i \right|^2 \right]^2} = \sum_i \eta_i + \frac{R^2 \sum_i \sum_{j+1} O_i O_j^*}{\left[\left(\sum_i t_i \right) R^2 + \sum_i t_i \left| O_i \right|^2 \right]^2} \quad (3-17)$$

That is there will be "interference terms" which could increase or decrease $\eta_1 - \sum \eta_i$. Since these are not predictable in general, we can at least get some idea of what is happening by assuming

$$\eta_1 = \sum_i \eta_i$$

$$\eta_1 \approx \sum_i \eta_i \quad ?$$

(3-18)

If $t_1 \gg t_i$ for all $i \neq 1$, the "correction terms" due to $i \neq 1$ exposures in the CMF have little effect on the diffraction efficiency. We list below η_1/η_0 for CMF's dominated by two MF's (1 and 2 by assumption), where η_0 is the single-exposure efficiency.

$K = ?$

what equation?

Now, what about t_1/t_2 ?

t_1/t_2	η_1/η_0
1	0.25
2 or 1/2	0.55
3 or 1/3	0.63
4 or 1/4	0.68
5 or 1/5	0.72
10 or 1/10	0.84

Likewise if there are three "big" terms t_1 , t_2 , and t_3 , we obtain results such as these.

$t_1:t_2:t_3$	η_1/η_0
1:1:1	0.11
1:1:0.5	0.36
1:0.5:0.5	0.38
1:0.5:0.2	0.45

We conclude that so long as only a few terms dominate the diffraction, efficiency of a CMF need not suffer drastically.

We now enquire about linearity. Here we encounter some subtle but important problems. We must distinguish between two cases. In Case 1 we have $K \gg 1$ at all points. The exposure is dominated by the reference beam intensity. In Case 2 we have K near or not much larger than 1 for some

spatial frequencies (indeed for those spatial frequencies which contribute most heavily to the readout not only by having "high" diffraction efficiencies but also by being illuminated by more light). These holograms have object-intensity-dependent exposure levels. When we operate with recording media of very limited dynamic range (as all holographic emulsions have), real problems come about. The spatial frequency regions from MF_1 which exceed the fog level depends on the other exposures. Likewise, the regions leading to saturation of MF_1 also depend on the other exposures. Thus the linearity assumption is violated.

These considerations lead us to prefer $K \gg 1$ for all exposures for linearity. But for $K \gg 1$,

$$n \approx \frac{1}{16K} \quad (3-19)$$

even for a single dominant MF. For three roughly-equal matched filters in the CMF,

$$n \approx \frac{1}{144K} \quad (3-20)$$

If $K = 10$, we have a maximum diffraction efficiency of roughly 0.07%. In other words, good linearity leads to very low diffraction efficiencies.

It is possible, in theory, to minimize these problems in very thick, highly-modulated, phase-only holograms, e.g. in dichromated gelatin. As yet, these holograms are too unpredictable and unstable to serve for CMF's.

The effect of $|\gamma| = 2$ is also important. Let us write

$$\gamma = -(2 + 2 \epsilon) \quad (3-19)$$

where ϵ is the deviation from ideality (i.e. $\gamma = -2$). Note that ϵ may be positive or negative and $|\epsilon|/2$ need not be small. Then

$$T = E^{-\gamma/2} = E \cdot E^\epsilon \quad (3-22)$$

While the first term (E) has the desired wavefront, the second term multiplies it by a variety of unpleasant terms quite familiar to holographers. We conclude that we must have $|\epsilon| < 1$ in order to predict CMF behavior from the MF behaviors. These nonlinearities can not be avoided in thick holograms by any technique. So, once again, they are unsuitable for CMF's.

4. EXPERIMENTAL RESULTS

As measured from the number of boxes of plates used, roughly 150 holograms were recorded and measured. The results are analyzed here.

4.1 K-Ratio and Dynamic Range

High K ratios led to disastrously low diffraction efficiencies as predicted in Section 3. These low diffraction efficiencies would be unacceptable for any practical applications.

K ratios near unity at the center gave the best compromise between diffraction efficiency and repeatability.

Lower K ratios led to a very interesting result. The autocorrelation diffraction efficiency became almost exposure independent. What happened (as revealed by microscopic examination of the holograms) was that at each exposure level a new band of spatial frequencies became important. Thus we predicted and observed greater variation in cross-correlation measurements. The higher exposures led to emphasis of higher spatial frequencies and hence to greater discrimination. What we are observing is the predicted "chopping" effects of the limited dynamic range of the recording medium.

4.2 Repeatability

Repeatability day to day was no worse than repeatability minute to minute so far as recording the hologram goes. A typical result is shown in Table 4-1. These resulted from five supposedly identical exposures at each exposure level over a two day period. We note the effects of dynamic range. The lower exposure holograms are more repeatable but (because they emphasize low spatial frequencies) less discriminating.

Another kind of nonrepeatability which was totally unexplained happened. The response curve for a given magnification varied with the angle of the object transparency. Furthermore, and equally baffling, the peak response of

response of a given hologram when plotted versus that rotation angle tended to peak as many as 20° away from the taking angle. This probably reflects target anisotropy combines with recording nonlinearity.

Table 4-1 Typical Variability

Exposure Time (m seconds)	Autocorrelation Signal (mw)	Variability
200	1.13 ± 0.15	13%
300	0.54 ± 0.20	37%
400	0.25 ± 0.05	32%

4.3 Additivity

The primary difficulty we observed (far worse than the poor repeatability) was a consistent failure of additivity. Our analysis (Section 3) suggested that nonlinearity effects ($\gamma = -2$, limited dynamic range) could produce such effects. Thus while the effects might be predictable in a detailed enough, object-dependent analysis, this effectively destroys the simple additivity assumption upon which the CMF was postulated. Figure 4.1 shows typical additivity results. We show here responses of MF's of tanks at two angles 30° apart and the same magnification. Calling those MF₁ and MF₂, we exposed to accomplish

$$CMF = 0.5 MF_1 + 0.5 MF_2 \quad .$$

Clearly simple additivity fails. In five different MF combinations, the CMF was unpredictable from the MF's.

4.4 Subtraction

Our best success story is subtraction. In Figure 4.2 we show a typical MF response versus angle curve and the curve for

$$CMF = 0.5 MF - 0.5 MF \quad .$$

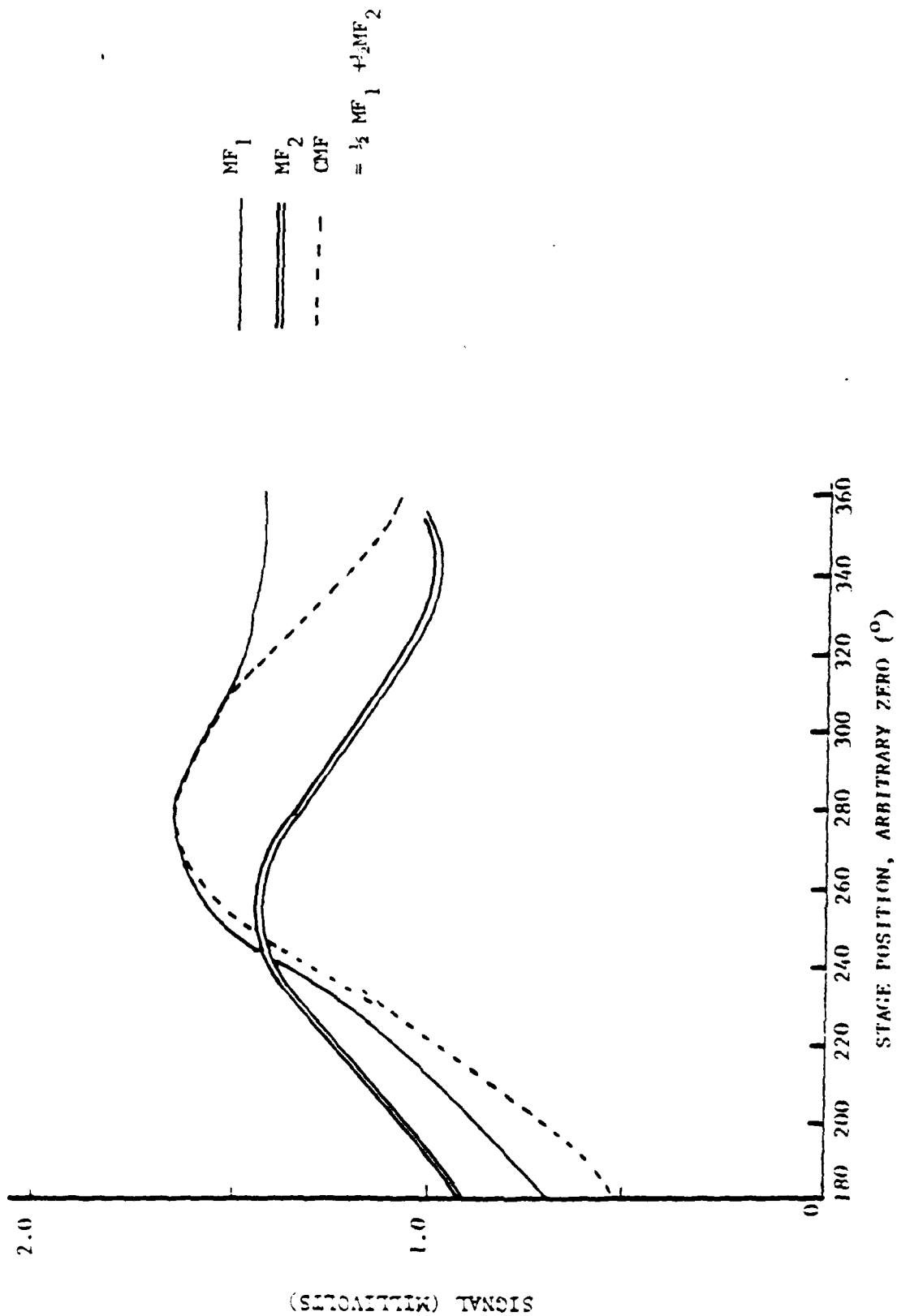


Figure 4.1. Typical Additivity Result

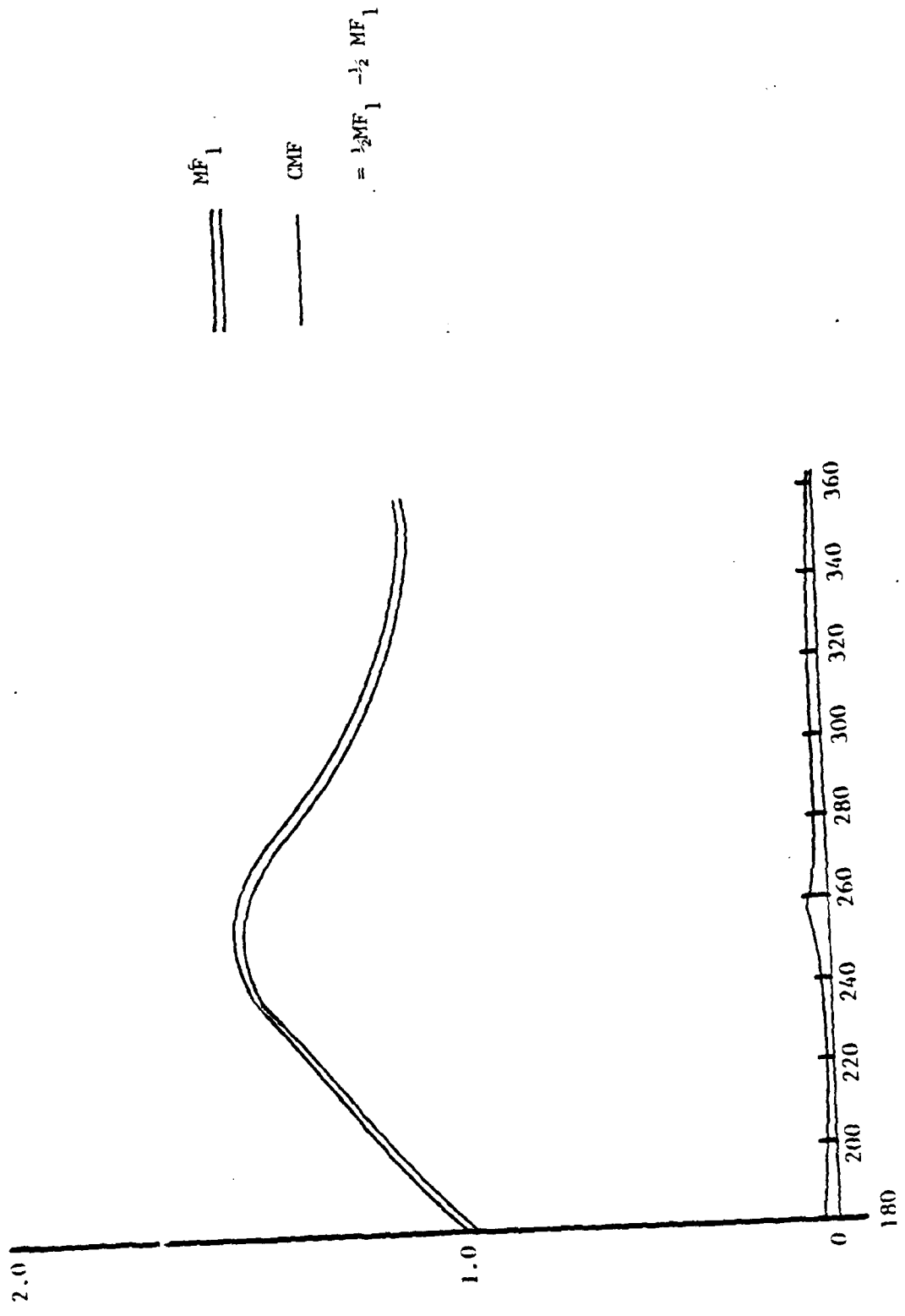


Figure 4.2. Typical Subtraction Result

5. CONCLUSIONS

Several conclusions follow from our theoretical and experimental studies. We list them here in no particular order.

First, the only adequate recording medium for CMF's would be highly repeatable (excluding dichromated gelatin immediately), linear ($|\gamma| = 2$ effectively though γ is not defined for a phase hologram), phase-only material. We do not know of such a material. Thick phase materials are inherently "nonlinear".

Second, CMF's on HRP material can have barely-adequate repeatability (approaching 10%) but fail completely in additivity by producing nonlinear results. Subtraction, however, is adequate for CMF production.

Third, recording CMF's even with an ideal recording medium is a difficult task at best. Laser stability, mechanical stability, realignment, and air currents are major problems.

Fourth, the CMF concept is attractive in principle but impractical for all presently-available media.

6. REFERENCES

1. H.J. Caulfield and D. Casasent, Opt. Eng. 19, 152 (1980).
2. H.J. Caulfield and R. Haimes, Appl. Opt. 19, 181 (1980).
3. H.J. Caulfield and W.T. Maloney, Appl. Opt. 8, 2354 (1969).
4. C.F. Hester and D. Casasent, Appl. Opt. 19, 1758 (1980).
5. J.R. Leger and S.H. Lee, Appl. Opt. 21, 274 (1982).
6. B. Breunecker, R. Hauck, and A.W. Lohman, Applied Optics, Vol. 18, 2746 (1979).
7. H.J. Caulfield and R. Haimes, Applied Optics, Vol. 19, p. 181 (1980).
8. H. Fujii and S.P. Almeida, Applied Optics, Vol. 18, p. 1659 (1979).
9. C. Hester and D. Casasent, Applied Optics, (to appear in June 1980).
10. D. Casasent and A. Furman, Applied Optics, Vol. 16, p. 1662 (1977).
11. D. Casasent and D. Munoz, Optical Pattern Recognition, SPIE Proceedings, Vol. 201, p. 58 (1979).
12. H.J. Caulfield, R. Haimes, and J. Homer, Isr. J. Technol. 18, 263 (1980).
13. H.J. Caulfield, J. Opt. Soc. Am. 58, 003 (1968).

APPENDIX
COMPONENTS LIST

Laser: Spectra-Physics Model 165, W/etalon, operated at 514.5 nm.

Fixed N.D.: Vacuum evaporated inconel on glass, nominal density = 1.3.

Shutter: Newport Research Model 846 HP (Tantalum Blade) controlled with
Newport Research Model 845 Controller 10 msec to 990 sec in 4
decades. Accuracy 0.05% \pm 10 μ sec.

Spatial Filter: Newport Research Model 900.
10 x objective lens, 25 μ m pinhole

Collimating Lens: 100 mm f/2

First Surface Mirrors (2): Vacuum evaporated aluminum on pyrex $\lambda/10$ surface

Removable N.D.: Wratten #96, nominal density 3.0

Liquid Gating Cell: Filled with n-butyl phthalate

Transform Lens: 68.5 cm f/10

Target Object: Positive photograph of tank on Type TE HI-Res Plate

Nikon Rotary Stage: Accurate to \pm 5 minutes of ARC

Location Jig: Pin fixtures permitting relocation accuracy of \pm 0.001 in.

$\lambda/2$ Retardation Plate: Karl Lambrecht Model WPOA-1-12-514.5 Air Saced,
Quartz, in rotary mount

Collection Lens: Nikon 75 mm f/2 NIKKOR-0

Photodetector: United Detector Technology Model 11A Photometer/Radiometer

END

FILMED

7-85

DTIC